Integrity of Adhesive Bonded Joints Using NDE of Ultrasonic Longitudinal Waves (Part 1: d-mode Technique)

E. E. Elgharib*, A. M. Abdelhay**, and M. I. Etman***
*Ph D Student and Assistant Lecturer at Faculty of Engineering, Helwan University,
** Professor of Engineering Mechanics, at Faculty of Engineering, Helwan University
*** Professor of Industrial Engineering, at Faculty of Engineering, Helwan University,

ABSTRACT

Adhesive integrity of bonded joint is one of the important issues of a large numbers of current literatures. This paper presents an analytical, numerical and experimental investigations for the adhesive material structural integrity of Single Lap Joints (SLJ). Non-Destructive Evaluation (NDE) using Ultrasonic Longitudinal Incident waves (ULW) was used for the process of evaluating, and assessing of adhesive material integrity for SLJs. A parameter named Spectral Attenuation Coefficient (SAC) was derived and proposed to be used for the required objective, in addition to three other UT parameters. NDE results of ultrasonic testing of single lap joints showed a quite dependency and sensitivity of the SAC parameter from different adhesive defects at different content levels. As a general trend for most of the NDE tested specimens, it was noticed that the measured SAC parameter, increases linearly up to a critical point, then suddenly change to a larger values.

Keywords:
Ultrasonics, NDE, adhesive integrity, single lap joints, Adhesive joints, spectral attenuation coefficient, spectral analysis.

1. Introduction

Adhesive bonding joints are simple in construction and manufacturing and in some engineering applications. Adhesive bonding joints are being increasingly used in structural applications, which are justified by their well-known advantages over the mechanical joints[1-6], such as substantial weight reduction compared to bolted and riveted joints, good stress distribution and hence stronger is the joint, provides a sealing function in addition to a fastening function, Dissimilar materials can be bonded, better fatigue properties, etc.

Health monitoring of adhesive joints by non-destructive techniques will be appropriate to inspect of their both performance and quality. Non-destructive techniques offer a wide range of methods; which can be customized to suite a specific application[7-9].

Ultrasonic non-destructive evaluation approaches still have been attractive and in demand for implementation to evaluate the quality of adhesive bonding. Unfortunately, no attempt was made of using the NDE of Ultrasonic Longitudinal normal incident Waves (ULW), specially Through transmission to check or evaluate adhesive bond integrity[10-14], so in this paper Ultrasonic (UT) parameters were suggested to be used in the assessment and evaluating process of adhesive material integrity for Single Lap Joints.

2. The Developed NDE Spectral Parameters

Applying the spectral analysis (FFT) of the captured UT time signal using the ULW in Through Transmission mode (ie. dual probes or shortly d-mode, where two ultrasonic probes are used). The propagation of longitudinal waves in solids is addressed in Wave Theory, where the solution of the wave equation is defined and well established [15-18]. Normally, the amplitude of the propagated longitudinal ultrasonic waves in the frequency domain is called “Spectral amplitude”. Such Spectral amplitude A(x,f) of the ultrasonic wave propagated through a homogeneous, isotropic and absorptive medium along a distance ***x*** (see Figure 1) can be described as a superposition of plane waves:

$$A\,(x\,,f\,) = G\,(f)\,.\,e^{[\,i\,(\,k\,x - 2\,\pi\,f\,t\,)]} \quad (1)$$

$$G\,(\,f\,)\; = \;(\,1 - \,e^{-tf_1}\,)\;\; e^{-tf_2} \quad (2)$$

el time. Since, the medium is absorptive; the wavenumber is a complex number:

$$k \;=\; k_r \;+\; i\;\alpha \qquad (3)$$

where k_r is the real part of the wavenumber, and α the attenuation coefficient in (neper /unit length):

$$\alpha = \;\frac{1}{x}\,\ln\frac{A(t)}{A_0} \qquad (4)$$

In this expression $\mathbf{A_0}$ is the unattenuated amplitude of the propagating time wave at some location. The amplitude **A** is the reduced amplitude after the wave has traveled a distance **x** from that initial location.

By Substituting (3.3) into (3.1) yields:

$$A\,(\,x\,,\;f\,) = G\,(f)\,.\,e^{[\,i\,(\,(k_r\,+\,i\;\alpha\,)\,x - 2\,\pi\,f\,t\,)]}$$

Or

$$A\,(\,x,\;f\;) = G\,(f)\,.\;e^{-\alpha\,x}\;\;.\,e^{[\,i\,(\,k_r\;x - 2\,\pi\,f\,t\,)]} \qquad (5)$$

where each frequency component f travels with the phase velocity $cp = \frac{2\,\pi\,f}{k_r}$.

Figure 1. shows a schematic diagram of three different layers of two adherends of d-thickness each, and an adhesive bond layer of Δ-thickness. An ultrasound pulse travels normally from the adherend bottom through the adhesive layer (with transmission coefficient T and reflection coefficient R) to the top adherend strip, and is reflected back to the bottom adherend.

Such Primary reflected pulse has traveled through a round trip of 2H (i.e. Total joint thickness H = 2 d + Δ), with frequency travel time of 2 t_H (i.e. t_H = H/C_p in frequency Domain, C_p is the Phase velocity)

The spectral amplitude of the Primary Reflection, indicated by B in shown in Fig 3.2 (s-mode) is:

Where f is the frequency, G(f) is the source pulse function; which is generated by the transducer or the ultrasonic probe, and can has the form[67]:

k is the wavenumber ($k = 2\pi f / c_p$) and t is the travel time. Since, the medium is absorptive; the wavenumber is a complex number:

$$A_1\,(\,x = 2H\,,\;f\;) = T_1^2\;T_2^2\,.\,G\,(f)\,.\;e^{-\alpha(\,2H\,)}\,.\,e^{[\,i\,(\,k_r\;(\,2\,H\,) - 2\,\pi\,f\,(2t_H)]} \qquad (6)$$

where T_1 and T_2 are the transmission coefficients for the adherend media and adhesive media respectively.

When the primary reflected pulse reaches the lower interface. It is reflected back to make a second round trip and reach the ultrasound probe as the First Reflection (see C-pulse in Fig 1 d-mode) of a series of multiple backwall reflections or echoes. This First Reflection has traveled a total of 3H in a time period of 3 t_H.

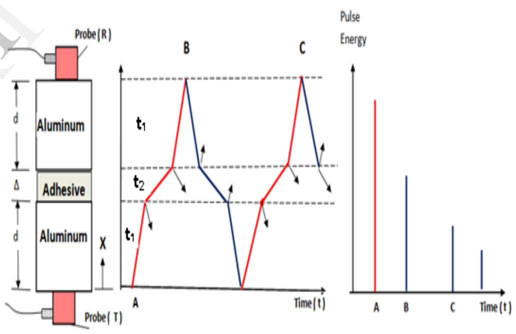

Figure 1. Major ultrasonic pulses in Through Transmission (T/R) UT technique (d-mode)
(A= Initial pulse, B= Primary Reflection, and C= First Reflection pulse)

The First Reflection shown in Figure 1. (d-mode) is a first-order reverberation or multiple reflection with spectral amplitude of:

$$A_2\,(\,x = 4H\,,\;f\;) = T_1^4\;T_2^4\,.\,G\,(f)\,.\;e^{-\alpha(\,4H\,)}\;\;.\,e^{[\,i\,(\,k_r\;(\,4\,H\,) - 2\,\pi\,f\,(4t_H)]} \qquad (7)$$

The ratio of the Fourier amplitudes is:

$$\left|\frac{A_2\,(f)}{A_1\,(f)}\right| = |T_1^2\;T_2^2\,|\;.\;e^{-2\,\alpha\,H}\;\;.\;\;e^{\,i\;[\;2\,K_r\,H - 4\,\pi\;f\;t_H]} \qquad (8)$$

But, since the phase velocity of reflected ultrasound pulse is: $cp = \frac{2\,\pi\,f}{k_r}$, last spectral amplitude ratio can be written as:

$$\left| \frac{A_2\,(f)}{A_1\,(f)} \right| = |T_1^2\ T_2^2|\ .\ e^{-2\,\alpha\,H}\ .\ e^{\,i\,[\,2\,K_r\,H\ -\ 2\,K_r\,C_p\,t_H]} \qquad (9)$$

Also, the reflected wave travel time for one-way trip in the frequency domain is $t_H = H/C_p$, which further simplify the last spectral amplitude ratio into:

$$\left| \frac{A_2\,(f)}{A_1\,(f)} \right| = |T_1^2\ T_2^2|\ .\ e^{-2\,\alpha\,H} \qquad (10)$$

Taking logarithm of two sides of (3.10),

$$ln \left| \frac{A_2\,(f)}{A_1\,(f)} \right| = ln\ |T_1^2\ T_2^2| \ -\ 2\,\alpha\,H \qquad (11)$$

Langton et al. [19] and Chaffai et al.[20] showed that the attenuation coefficient (α) only accounts for the absorption and is assumed to depend linearly on frequency, i.e.

$$\alpha\ =\ K\,.f \qquad (12)$$

Where, K is the constant of proportionality, thus, Eq (11) can be written as:

$$ln \left| \frac{A_2\,(f)}{A_1\,(f)} \right| = ln\ |T_1^2\ T_2^2|\ -\ (2\,K\,H\,)\ f \qquad (13)$$

Or

$$ln \left| \frac{A_2\,(f)}{A_1\,(f)} \right| = a - b\,f \qquad (14)$$

This last equation, states that " The Logarithmic of the Spectral Ratio is a function of the Frequency, and is presented by a Straight Line, as shown in Figure 2. with:

a Slope $b = -2\,K\,H$, (15)

and intercept $a = ln\ |T_1^2\ T_2^2|$ (16)

This Spectral Attenuation Coefficient, or shortly SAC, can be used to assess, evaluate and monitor the Integrity of the adhesive bond material.

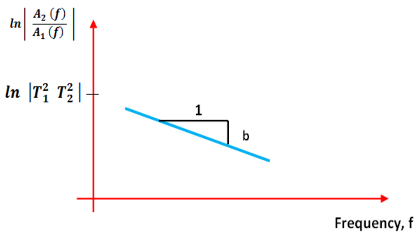

Figure 2. Representation of the Spectral Attenuation Coefficient (SAC) as a function of Frequency by Linear Relationship

3.4 Computational Procedure

Algorithm for the computational sequences is shown in Figure 3. as a flow chart. This algorithm is an initial proposal and subjects to modification according to the Design of Experiment presented in the next chapter. Matlab software is going to be extensively used for the proposed numerical technique. Fast Fourier Transformation (FFT) is mainly the mathematical tool; which can be used to convert the acquired Ultrasonic normal incident Time Signal from the Time Domain into the Frequency Domain.

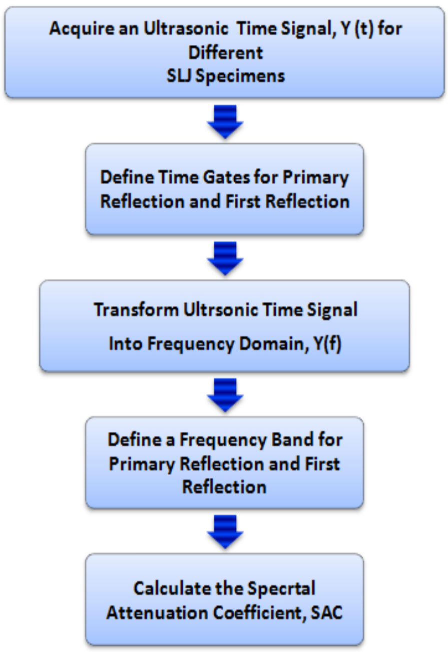

Figure 3. Computational Flow Chart for the Determination of SAC for each NDE Specimen

In the numerical analysis of acquired NDE time signal, time gates of equal lengths have to be defined for the two segments of the Primary Reflection and First Reflection segments. Also, in the frequency domain, not all the frequency components are used for the least – squared fitting but only the frequency range corresponding to the linear portion of the curve is employed. Visually, a frequency band is selected corresponds to a linear portion of the curve of negative slope, see Eq (15), and can be automated using a Matlab code.

3.5 NORMALIZATION OF SAC

In order to observe only the changes in Ultrasonic incident normal time signal due to adhesive integrity, a normalization process was suggested and applied to make NDE results are independent to the initial condition of the three main elements of adhesive bonded joint. Normalizing process was to exclude any changes from both of the adherend condition and adhesive initial condition. By looking into Eq (14), one can perform such a normalization by dividing both the denominator and numerator of the left hand ratio of spectral amplitude by their corresponding ZERO load segments in the frequency domain; such as:

$$ln\left|\frac{A_2\,(f)\;/\,A_{02}\,(f)}{A_1\,(f)\,/\,A_{01}\,(f)}\right| = a - b\,f \qquad (17)$$

Thus, any changes in the NDE signal is attributed only to the changes in integrity of the adhesive material condition.

Additionally, three other UT parameters are proposed for non-destructively evaluate the adhesive material integrity. These employed UT parameters are: Maximum spectral amplitude ($FFT|Y|_{max}$), Frequency at maximum FFT (f_m), and Phase Shift Angle at maximum FFT (Θ_m).

3. Experimental Setup

3.1 Adhesive and Adherend Materials

Tested specimens in the form of Single Lap Joint (SLJ); each consists of three parts; two adherend strips from Aluminium alloy(AW-1350-H12) bonded together with the adhesive material (Devcon-Fasmetal-10), as schematically shown in Figure 4.

Surface preparation of debarring of all edges and polishing of bonding are with 400 grit sandpaper was followed, with average resulted measured surface roughness of Rq=1.4075±0.147 µm (Ra=1.065±0.057 µm) Special attention was paid to remove any surface contaminants that would later degrade the adhesive bond.

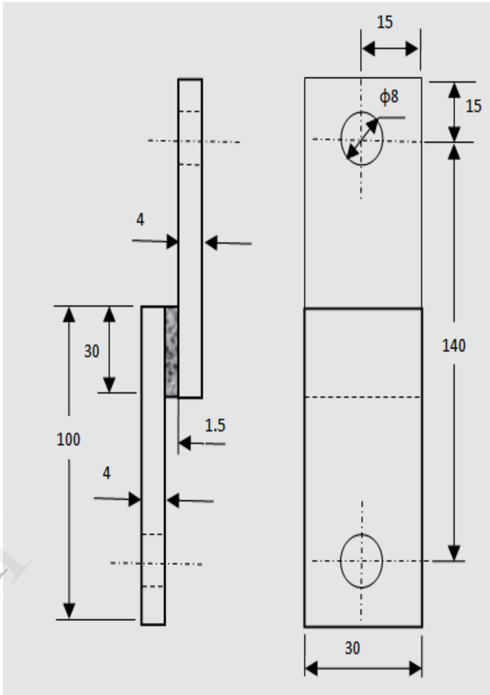

Figure 4. Main dimensions of SLJ specimens

3.2Artificially Induced Defect Types

Adhesive structural integrity can be disturbed by the existence of one or more internal flaws or defects; which can affect their service performance and in general the joint integrity in the first place.

Three types of defects, are artificially simulated using, polystyrene patches of 5.5 mm diameters for adhesive disband or Type-1 defect. Interlaminar defects as a form of macro-crack is simulated by rectangular layers of 0.1 mm thickness plastic foils, to represent Type-2 defects. Finally, rubber foams were used to generate voids in the adhesive structure(as shown in figure 5.). These defect types were chosen to control their existence percentage along the adhesive/adherend interface or within the adhesive structure.

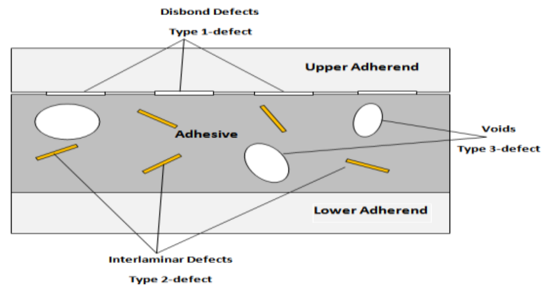

Figure 5. Schematic sketch for some potential adhesive bonded joint defects

3.3 Testing Equipment and Instrumentations

Non- destructive testing of SLJ specimens using Ultrasonic Technique (UT) of Normal incident waves was carried out using special design loading device Figure 6.

This device is equipped with a Digital measuring load system (N/N A201020 Type Ze . B 5 KN capacity Load cell model + LCD with signal processor xk 3190 - A19E- Model with 3KN Range and 0.20 N resolution).

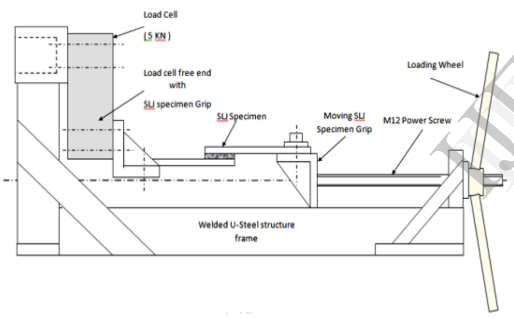

Figure 6. Schematic layout of the of the specially designed loading device

From experiment design the modes of ultrasonic techniques was proposed Through Transmission Technique. In Through - Transmission ultrasonic technique, a Dual Probes are used; where one is used to send and the other to receive Normal incident waves of ultrasonic pulses, shortly hereafter is referred by " d ".

3.3.1 NDE Experimental Testing Procedures; Figure 7. illustrates the experimental set-up; which is primarily based on the flow chart of Fig 8. Non-destructive evaluation (NDE) of the SLJ specimens is started at zero applied load, then incrementally increased by 250 N up to the fracture maximum load. At each load, started from the reference zero load, the analogue time signal Y(t) displayed on the screen of the Ultrasonic Equipment (NDT 801D-model) was transferred to the two channels digital storage oscilloscope (Tektronix TDS 210–60MHz/1 G s/s model).

Acquired Ultrasonic Time Signal Y(t) was digitally displayed on the screen of the oscilloscope (TDS 210) and simultaneously processed by DELL – Core i7 Laptop computer; where a MatLab code (ScopeGUI) is running to acquire the resulted ultrasonic time signal Y(t).

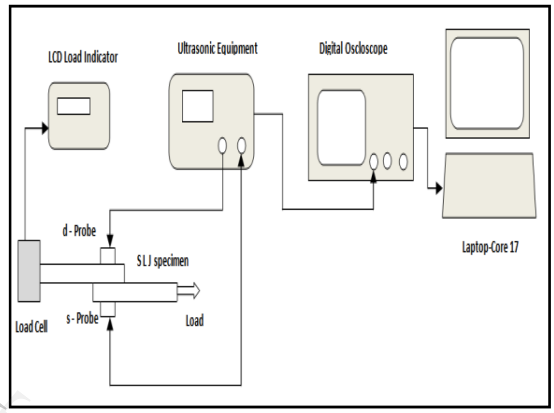

Figure 7. Schematic experimental set-up

3.3.2 NDE Data Processing; For each type of tested SLJ specimen, recorded and stored data from the ZERO load (A Reference data) and each consecutive load up to the fracture point was processed according to the flow chart seen in Figure 8.

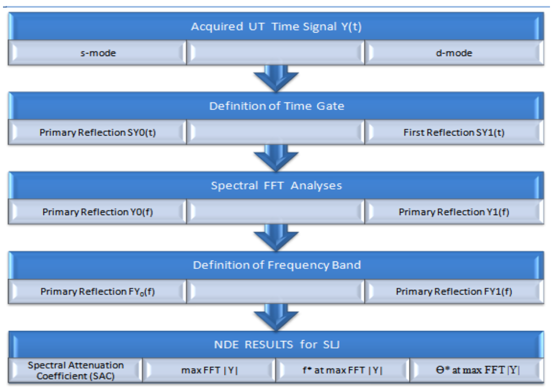

Figure 8. A flow chart for Data Collection and Data Reduction

The application of numerical data reduction was gone through 5 stages, as illustrated in Figure 8. The graphical representation of such numerical data manipulation and processes were illustrated in

Figure 9. for d-mode specimens. A group of Matlab codes were programmed and especially customized to suite this jobs this code for the d-mode tested specimens.

Time gates for Primary and First reflection pulses were defined for d-mode tests, through careful study of the NDE ultrasonic time signal. Table 1 lists these time gate values. Also, Table 1. includes the Frequency bands that are needed in the numerical manipulations of the spectral FFT analyses. Spectral Attenuation Coefficient (SAC), proposed by Eq (17) was the main target of this numerical analysis.

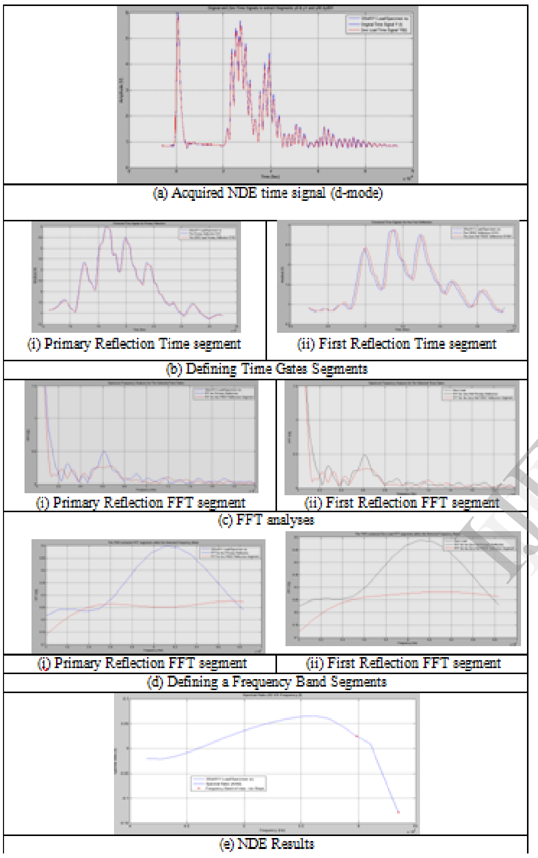

Figure 9. Graphical representation of Data Reduction for the NDE of SLJ specimen no. 011 at 3.5 KN applied load (d-mode)

Table 1. NDE Time Gates and Frequency Bands

	d- mode NDE	
	Primary Reflection	Primary Reflection
Time Gates, (µS)	2.0 – 3.28	3.28 – 4.53
Frequency Band, (MHz)	4.15-6.50	4.15 – 6.50

4. Results and Discussion

4.1 Adhesive Integrity And Spectral Attenuation Coefficient (Sac)

Different NDE test results are presented in Figure 10. through Figure 11. The following remarks can be highlighted for each type of tested Single Lap Joint(SLJ).

4.1.1 Specimen 111 (Defect-Free); Examining Figure 10. it is noticed that for d-mode SAC less sensitive to change with shear stress (-1 mean value), with appreciable increase in SAC of - 4 at the fracture point.

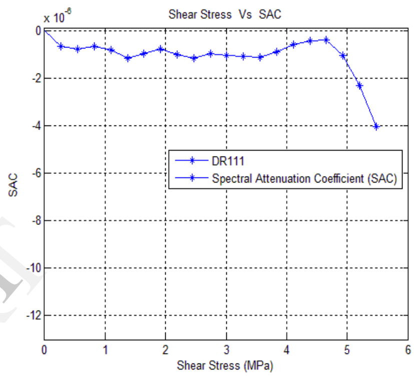

Figure 10. Effects of adhesive integrity on SAC for SLJ no. 111

4.1.2 Specimen 02X(Type 2-Defect); In general, interlaminar defect with different ratios (1%, 2% and 3% by volume of total adhesive material volume) in Figure 11. have showed an increase (i.e. negatively) in SAC with shear stress. Near to the fracture stress, a sudden change in SAC is noticed for d-mode of ultrasonic testing.

Also, it is noticed that in d-mode the rate of increase in SAC with the increase in shear stress is in continuous with increasing the effect levels. It seems that this type of interlaminar defects has a bigger influence on strength at higher content of defect ratios.

All NDE tested specimens of SLJs have shown rapid increase in SAC due to the higher attenuation caused by scattering along these laminates within the adhesive structure material. Such scattering at lower defect level is bigger due to unreturned ultrasonic waves to its source (i.e. the probe).

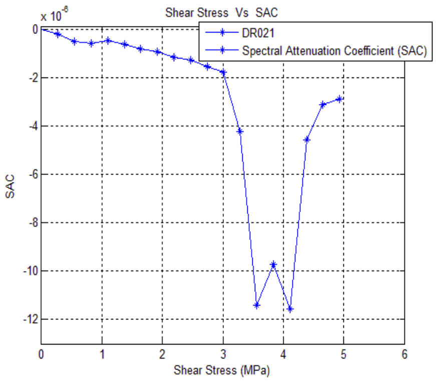

SLJ no. 021

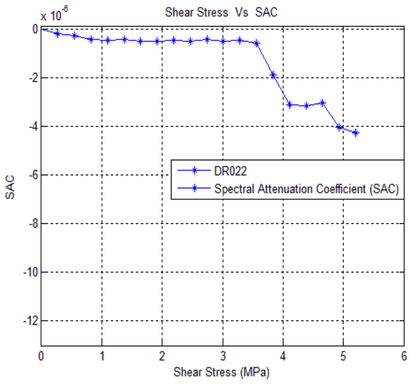

SLJ no. 022

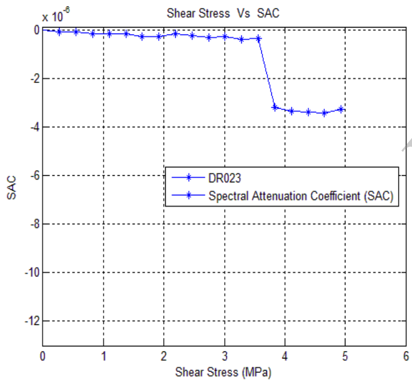

SLJ no. 023

Figure 11. Effects of adhesive integrity on SAC for SLJ

4.2 ADHESIVE INTEGRITY AND MAXIMUM AMPLITUDE OF FFT|Y|$_{max}$

From spectral analysis of the NDE ultrasonic signal (see Figure 9. (c)), the maximum observed spectral amplitude, A(f) or FFT|Y|$_{max}$ for the whole frequency spectrum is used here to show their relations with the type of induced defect and its percent content. The FFT analysis for the Primary Reflection is used, since results from First Reflection is similar but with lower values.

4.2.1 Specimen 111 (Defect-Free); For both NDE modes of testing, the FFT|Y|$_{max}$ remain almost leveled at 0.4 for s-mode and 0.6 for d-mode, as shown in Figure 12. Near to the fracture shear stress the FFT|Y|$_{max}$ starts to suddenly drop down, d-mode specimens have a higher drop rate.

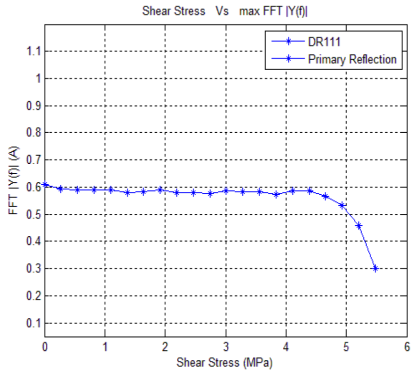

Figure 12. Effects of adhesive integrity on FFT|Y| for SLJ no. 111

4.2.2 Specimen 02X(Type 2-Defect);Same behavior were observed for type 2-defect, as shown in Figure 13., where the FFT|Y|$_{max}$ remains leveled for each level of defect percent, 0.88 for d-mode. Sudden drop in amplitude was observed at 3 MPa, 3.8 MPa, and 3.6 MPa for different levels of defects and almost the same for d-mode. The rate of drop was higher for d-mode. This drop in amplitude can be a measure for near fracture condition for the loaded SLJ.

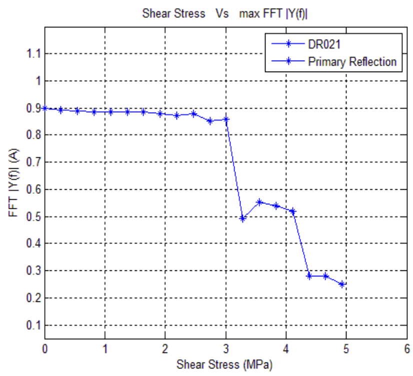

SLJ no. 021

Figure 13. Effects of adhesive integrity on FFT|Y| for SLJ

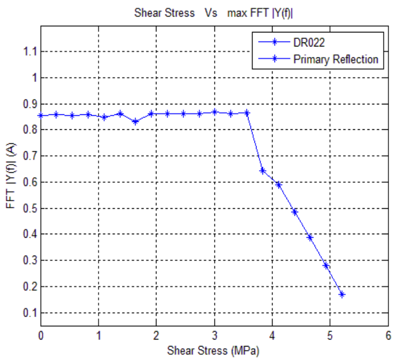

SLJ no. 022

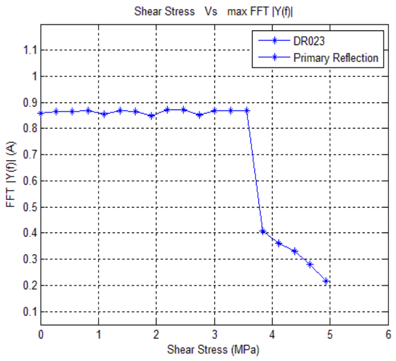

SLJ no. 023

Figure 13. (cont.) Effects of adhesive integrity on FFT|Y| for SLJ

4.3 ADHESIVE INTEGRITY AND FREQUENCY AT FFT|Y|$_{max}$

Dominant frequency of maximum amplitude is another variable which can be used to characterize adhesive integrity. This frequency is obtained from the spectrum diagram (c) of Figure 9. for d-mode,

4.3.1 Specimen 111 (Defect-Free); For NDE d-modes of testing (Figure 14.), the FREQUENCY remains almost leveled at 4.4 MHz for d-mode.

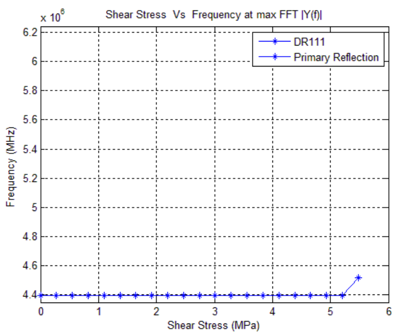

Figure 14. Effects of adhesive integrity on FREQUENCY for SLJ no. 111

4.3.2 Specimen 02X(Type 2-Defect); Frequency at maximum (FFT|Y|$_{max}$) remains leveled for all levels of defect at frequencies of 4.9, 4.9, and 5 MHz for level 3 defect, see Figure 15. for the d-mode, were observed for different defect percent respectively. Changes in these frequencies start to show up at 3.0, 3.8 and 4.1 MPa for different defect level in sequence.

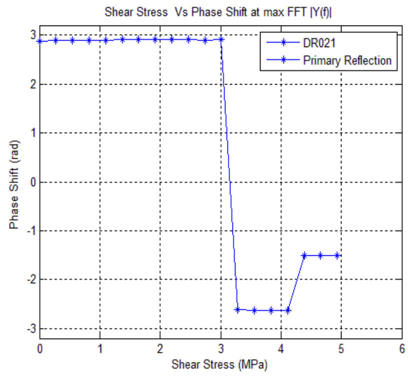

SLJ no. 021

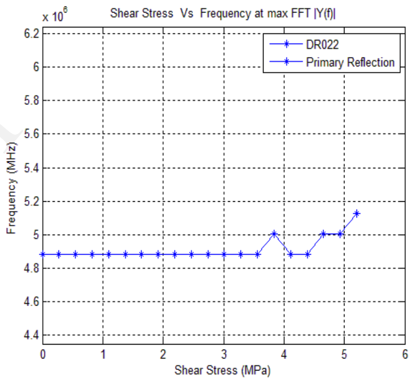

SLJ no. 022

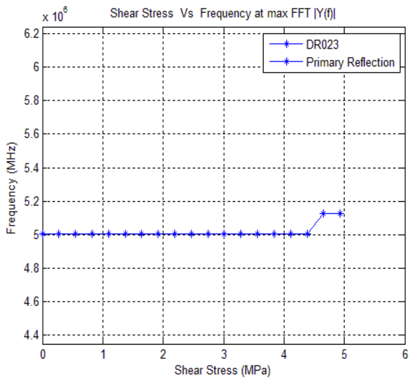

SLJ no. 023

Figure 15. Effects of adhesive integrity on FREQUENCY for SLJ

4.4 ADHESIVE INTEGRITY AND PHASE ANGLE SHIFT AT FFT|Y|$_{max}$

Applying the FFT analysis on the Primary Reflection ultrasonic pulse segment, its decomposed sine component signal can be lead or lag compared to the original signal of the NDE ultrasonic wave. Such phase shift angle for most dominant frequency of FFT|Y|$_{max}$ is another variable, which can be used for assessment and monitor adhesive bonded joints for any lack of integrity.

4.4.1 Specimen 111 (Defect-Free); As one can notice from Figure 16. that for NDE d-mode of testing, the Phase Angle_remain almost leveled at -1.4 rad for d-mode. The sudden change was noticed prior to fracture stress.

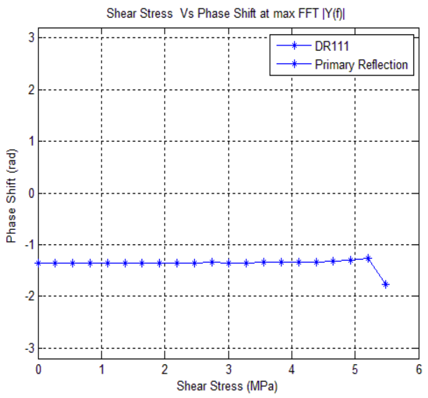

Figure 16. Effects of adhesive integrity on PHASE ANGLE SHIFT for SLJ no. 111

4.4.2 Specimen 02X(Type 2-Defect); Measured results of Phase Angle at maximum amplitude, plotted in Figure 17. revealed a similar behavior as for type 1-defect. For tested SLJ specimens d-mode, 2.9 rad for levels 1 and 2, and 2.1 rad for level 3 defect. Sudden change in phase angle was noticed for all specimens and at all levels.

5. Conclusion

NDE results of ultrasonic testing of single lap joints showed a quite dependency and sensitivity of the SAC parameter from different adhesive defects at different content levels. As a general trend for most of the NDE tested specimens, it was noticed that the measured SAC parameter, increases linearly up to a critical point, then suddenly change to a larger values. This behavior was illustrated in terms of the acting shear stress along the adhesive bonded joint. The other UT parameters were found to hold unchanged or invariable up to the same critical point for the SAC parameter, then a drop was exhibited.

The proposed methodology addressed in this work is expected to be highly beneficial for engineering applications to non-destructively evaluate and inspect the adhesive bonded joint integrity. Also, in-service inspection for adhesive bonded joints, using NDE technique, would be much more easier and effective.

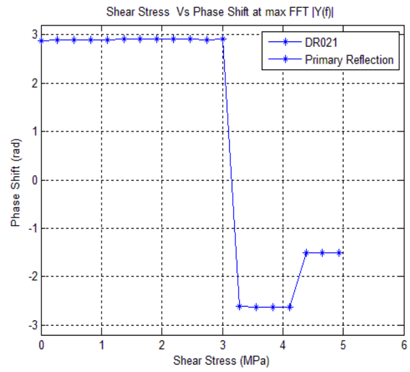

SLJ no. 021

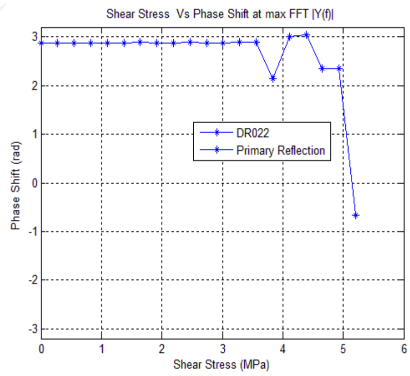

SLJ no. 022

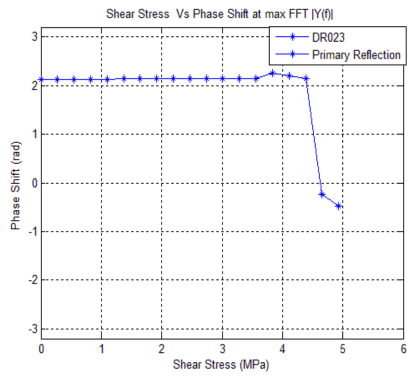

SLJ no. 023

Figure 17. Effects of adhesive integrity on PHASE ANGLE SHIFT for SLJ

Acknowledgement

The authors wish to thank the staff members of the Mechanical Engineering laboratories at Helwan University, Cairo University, and The Central Metallurgical Research and Development Institute (CMRDI) at Tebbin-Helwan. Also, thanks are due to Eng Mohamed Elsayed, at Mechatronic Department, Helwan University for his valuable assistance.

References

[1] A. M. Abdelhay, A. Hegazy, E. E. Elgharieb, "Comparative Experimental Study For Adhesive Bonding Joints" Production Engineering & Design For Development, PEDD7, Cairo, February 7 – 9, (2006) pp. 612-623.

[2] L.F.M Da Silva and Adams R.D, "The strength of adhesively bonded T-joints" International Journal of Adhesion & Adhesives 22 (2002) pp. 311–315.

[3] A. Al-Samhan and S.M.H. Darwish, "Strength prediction of weld-bonded joints" International Journal of Adhesion & Adhesives 23 (2003) pp. 23–28.

[4] D.W. Seo and J.K. Lim, " Tensile, bending and shear strength distributions of adhesive-bonded butt joint specimens " Composites Science and Technology 65 (2005) pp.1421–1427.

[5] A. Chadegani and R.C. Batra, " Analysis of adhesive-bonded single-lap joint with an interfacial crack and a void " International Journal of Adhesion & Adhesives 31 (2011) pp. 455–465.

[6] S. Azari, W. Oudad, A. Albedah, F. Benyahia, M. Belhouari, "Fracture load predictions and measurements for highly toughened epoxy adhesive joints" Engineering Fracture Mechanics 76 (2009) pp. 2039–2055.

[7] A. M Abdelhay, O. M. Dawood, A. Bassuni, E. A. Elhalawany, M. A. Mustafa, " A Newly Developed Cruciform Specimens Geometry for Biaxial Stress Evaluation Using NDE " AEROSPACE SCIENCES & AVIATION TECHNOLOGY, ASAT- 13, May 26 – 28, (2009) Paper: ASAT-13-TE-12.

[8] Z. Su, Lin Ye, Y. Lu, "Guided Lamb waves for identification of damage in composite structures: A review" Journal of Sound and Vibration 295 (2006) pp. 753–780.

[9] R. Mactabi, I. D. Rosca, V. H Suong., "Monitoring the integrity of adhesive joints during fatigue loading using carbon nanotubes" Composites Science and Technology 78 (2013) pp. 1–9.

[10] T. Kang, H.-H. Kim, S.-J. Song, H.-J. Kim, "Characterization of fatigue damage of Al6061-T6 with ultrasound " NDT&E International 52 (2012) pp. 51–56.

[11] H.-Y. Yeh and J.-H. Cheng "NDE of metal damage: ultrasonics with a damage mechanics model" International Journal of Solids and Structures 40(2003) pp. 7285–7298.

[12] Goglio L, and Rossetto M "Ultrasonic testing of adhesive bonds of thin metal sheets" NDT&E International 32 (1999) pp. 323–331.

[13] D.W. Schindel "Air-coupled ultrasonic measurements of adhesively bonded multi-layer structures " Ultrasonics 37 (1999) pp. 185–200.

[14] K. Imielinska, M. Castaings, R. Wojtyra, J. Haras, E. Le Clezio, B. Hosten, " Air-coupled ultrasonic C-scan technique in impact response testing of carbon fibre and hybrid: glass, carbon and Kevlar/epoxy composites" Journal of Materials Processing Technology 157–158 (2004) pp. 513–522.

[15] L.D. Broglie, "An Introduction To The Study Of Wave Mechanics" METHUEN CO. LTD. 36 ESSEX Street. W.C. First Published in 1930.

[16] C M. Langton, A V. Ali, C. M. Riggs, G. P. Evans, W. Bonfield ,"A contact method for the assessment of ultrasonic velocity and broadband attenuation in cortical and cancellous bone" Clin. Phys. Physiol. Meas. 11 pp. 243–9.

[17] R. Zheng, H. Le. Lawrence, D. S. Mauricio, L. Edmond, T. Dean, "Spectral ratio method to estimate broadband ultrasound attenuation of cortical bones in vitro using multiple reflections" Phys. Med. Biol. 52 (2007) pp. 5855–5869.

[18] J. G Proakis and D. G. Manolikis, "Digital Signal Processing", Printice -Hall, Inc. of India, New Delhi, 2004.

[19] S. Chaffai, F. Padilla, G. Berger, P. Laugier "In vitro measurement of the frequency-dependent attenuation in cancellous bone between 0.2 and 2 MHz" J. Acoust. Soc. Am. P 2000 (108) pp. 1281–9.

[20] J. krautkraemer and H. krautkraemer "Ultrasonic Testing of Materials" Translation of the revised second edition, springer International student, springer-verlage Berlin Heildelberg , New York, 1969.

[21] J.M. Allin, P. Cawley, M.J.S. Lowe,"Adhesive disbond detection of automotive components using first mode ultrasonic resonance "NDT&E International 36 (2003) pp. 503–514.

LIST OF SYMBOLS AND ABBREVIATION

Latin Alphabet

A	:	Initial pulse
A(x,f)	:	Spectral amplitude of the ultrasonic wave
A_{FFT}	:	Maximum FFT amplitude
A_0	:	unattenuated amplitude
$A_1(\boldsymbol{f})$	:	Amplitude of the Primary Reflected wave
$A_2(\boldsymbol{f})$	:	Amplitude of the First Reflected wave
B	:	Primary Reflection
b	:	Slope
C	:	First Reflection pulse
$\boldsymbol{c_p}$	:	phase velocity
d	:	an Adherend thickness
d-mode	:	Dual Probes (Through Transmission Techniques T/R)
FFT	:	Fast Fourier Transformation
$\boldsymbol{f}$	:	the frequency
f_m	:	Frequency at maximum FFT
$G(\boldsymbol{f})$	:	the source pulse function
H	:	Total joint thickness ($H = 2\,d + \Delta$)
K	:	the constant of proportionality
$\boldsymbol{k}$	:	the wavenumber
kr	:	the real part of the wavenumber
M	:	Mode of Ultrasonic Technique
NDE	:	non-destructive Evaluation
R	:	reflection coefficient
Ra	:	surface roughness (RMS), microns
Rq	:	surface roughness, microns
R1	:	Reflection coefficients for the adherend
R2	:	Reflection coefficients for the adhesive media
SAC	:	Spectral Attenuation Coefficient
SLJ	:	Single Lab Joint
T	:	transmission coefficient
T/R	:	UT Through Transmission technique (d-mode)
T_1	:	transmission coefficients for the adherend media
T_2	:	transmission coefficients for the adhesive media
t	:	travel time
t_H	:	Frequency Mean Travel Time for one way trip
ULW	:	Ultrasonic Longitudinal Waves
UT	:	Ultrasonic Testing
X	:	traveled Wave path distance
Y(f)	:	frequency domain
Y(t)	:	ultrasound time wave
Z	:	Acoustic Impedance

Greek symbols

Δ	:	an adhesive bond layer thickness
α	:	
Θ_m	:	Phase Shift Angle at maximum FFT
τ_{max}	:	Fracture Shear Stress (MPa)
01	:	type 1 defect
02	:	type 2 defect
03	:	type 3 defect